Elastic properties of solids containing elliptic cracks

Stefano Giordano* and Luciano Colombo†
Department of Physics of the University of Cagliari and Sardinian Laboratory for Computational Materials Science (SLACS, INFM-CNR), Cittadella Universitaria, I-09042 Monserrato (Ca), Italy
(Received 19 October 2007; published 21 February 2008)

We investigate the elastic properties of multicracked solids by considering dispersions of elliptic cracks with arbitrary nonrandom orientational distributions. We provide a unified theory covering all of the possible orientational distributions, ranging from the totally random one to the distribution where cracks are preferentially oriented in a given direction. We especially focus on the orthorhombic symmetry and transversely isotropic symmetry for the cracks distribution. In both cases, the elastic behavior is proved to depend upon the density of cracks and upon some order parameters. Finally, the regime of large crack density and isotropic orientation is studied by means of iterated homogenization and it is shown that the effective elastic moduli depend exponentially on the crack density.

DOI: 10.1103/PhysRevB.77.054106 PACS number(s): 62.20.M−, 46.50.+a, 62.20.D−

I. INTRODUCTION

It is widely accepted that the macroscopic degradation of materials is caused by the generation and the propagation of cracks and by their mutual mechanical interactions. In this context, the term degradation indicates the toughness reduction of a given material (or, more precisely, the reduction of its effective Young modulus). The linear elastic fracture mechanics (LEFM) provides the understanding of the failure instability[1] and the mechanical behavior of a single crack. LEFM results[2] are widely used and they have been recently validated by atomistic simulations.[3] The knowledge of the behavior of a single crack is, however, insufficient to predict the macroscopic properties of a multicracked medium. In fact, its overall mechanical behavior depends upon the positional and orientational statistical distribution of the assembly of cracks.

When we take into consideration the complex structure of a multicracked material, the central issue is to evaluate its effective stiffness tensor. This problem belongs to the field of homogenization techniques, where the effective elastic properties of composites depend on the elastic constants, the volume fractions and the spatial arrangements (i.e., microstructure) of their constituents.[4,5] The relative importance of these features is complicated, but some general rules may be inferred.[6] From the historical point of view, the most widely studied elastic homogenization theory is addressed to the case of a dilute dispersion of spherical or ellipsoidal inclusions into a solid matrix.[7,8] The corresponding results have been further generalized to large volume fraction values by means of the iterated homogenization technique[9] or by the differential effective medium theory.[10,11] The predictions of homogenization techniques are of great importance in several fields, ranging from materials science, to geophysics, to biomechanics. For example, interesting applications have been developed for rocks, where cracking is originated by several geological processes, like thermal gradients or tectonic stresses.[12,13] In addition, homogenization techniques have been applied to investigate the nonisotropic fracture mechanisms in mineralized biological tissues, like bone and dentin.[14,15]

A homogenization technique is adopted in the present study to understand the effects on the elastic behavior of a solid body due to a population of elliptic cracks with a given statistical distribution of orientations. The elliptic shape represents the most general geometry of a crack, as indeed observed in real samples. Furthermore, the elliptic shape allows us to analyze two important limiting cases, namely the so-called slit crack (or Griffith crack) and the circular crack. They are both paradigmatically important in fracture mechanics.[16,17] Under this respect, the present investigation provides a very general conceptual framework, including previously investigated specific cases.

In order to model the elliptic flat shape of a crack, we adopt an ellipsoidal void with an infinitesimally short axis. Treating the crack as a vacuous oblate ellipsoid of vanishing eccentricity is very convenient since it is possible to derive fully analytically the actual expression for any relevant elastic field, as also found elsewhere for simpler configurations.[18–20] As for the orientational distribution of cracks, so far basically only two possible distributions have been investigated: Cracks aligned with a given direction (order) or cracks uniformly oriented in the space (disorder). However, recent experimental reports indicate that a scattered angular distribution of cracks can produce sizeable effects on the effective elastic properties.[21,22] Therefore, the goal of the present paper is to analyze a multicracked solid with an arbitrary angular distribution of elliptic cracks. We take into account all the intermediate configurations between order and disorder (including the important case of a material with only partially aligned cracks) for two different distributions, namely the orthorhombic and the transversely isotropic one. They are both very important for practical applications. As a matter of fact, the orthorhombic case describes several processes in rocks and bones degradation,[12,14] while the transversely isotropic symmetry is more typical of material science like, e.g., in plasma sprayed ceramic coatings.[22]

The geometry of a single elliptic crack is shown in Fig. 1. To describe the orthorhombic case we can image an assembly of elliptic cracks generated by rotations around the x_1 axis, with a given arbitrary statistical angular distribution (see Sec. IV). The transversely isotropic case is, in turn, described by a population of elliptic cracks randomly oriented

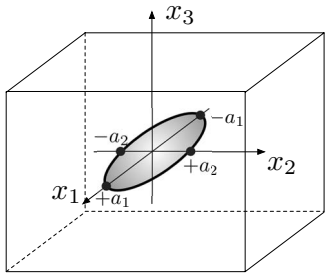

FIG. 1. Geometry of an elliptic crack (with aspect ratio $g=a_2/a_1$) lying in the (x_1,x_2) plane and embedded into an elastic medium with Young modulus E and Poisson ration ν.

in the space, and described by a given probability density for the angle between the normal vector to each crack and the x_3 axis (principal axis of the system; see Sec. V). In both cases, the angular distribution is described by a couple of order parameters.

Before developing our model, we like to provide some general comments about the homogenization procedure and the constitutive hypotheses underlying the present work. The first step of the theory (in both geometrical configurations) develops a homogenization procedure under the hypotheses of small crack density, so that the cracks are not interacting with each other. This simplifying assumption has been initially introduced in order to focus the attention on the effects of the orientational distribution of cracks. Our theoretical framework is then generalized by means of the iterative homogenizations method[9] which converges to the differential effective medium theory.[10] These more refined methodologies properly take into account the interactions among the cracks. It has been verified in several contexts that such homogenization procedures capture the trend of experimental data obtained on real materials.[5,11]

As for the basic hypotheses we remark that the present work is developed within the LEFM which is intrinsically scale-invariant. Therefore, it does not take into account the actual size of the objects involved in the modeling. In order to introduce the scale size, one should perform an atomistic simulation of the system, properly describing the actual interatomic distances and the effective lengths of the objects.[3] Furthermore, we have not considered many nonlinear phenomena occurring in fracture mechanics, especially at the crack tip zones where high stress intensities do not allow us to consider linear constitutive equations for the material.[2]

The paper is organized as follows. In Sec. II we develop the original formal procedure (based on the Eshelby theory) to calculate the strain field induced by a single ellipsoidal void with vanishing eccentricity. In Sec. III we describe the generalized methodology used to determine the effective (macroscopic) elastic tensor for a multicracked body. Finally, in Secs. IV and V we thoroughly discuss the case of orthorhombic and transversely isotropic symmetry, respectively.

II. SINGLE ELLIPSOIDAL VOID

Before introducing cracks, an isotropic and homogeneous solid matrix is characterized by the relation $\hat{T}=\hat{\mathcal{C}}\hat{\epsilon}$ (or, in components: $T_{ij}=\mathcal{C}_{ijkl}\epsilon_{kl}$), where $\hat{T}$ is the stress tensor, $\hat{\epsilon}$ is the strain tensor, and $\hat{\mathcal{C}}$ is the stiffness tensor. We adopt the Voigt notation (hereafter labeled by the tilde sign), defining the strain vector $\tilde{\epsilon}$ as

$$\tilde{\epsilon}=[\epsilon_{11}\quad \epsilon_{22}\quad \epsilon_{33}\quad \epsilon_{12}\quad \epsilon_{23}\quad \epsilon_{13}]^T \tag{1}$$

and the stress vector as

$$\tilde{T}=[T_{11}\quad T_{22}\quad T_{33}\quad T_{12}\quad T_{23}\quad T_{13}]^T, \tag{2}$$

where $(\cdot)^T$ means transposed. The stiffness tensor $\tilde{\mathcal{C}}$ for the perfect solid is therefore

$$\tilde{\mathcal{C}}=\begin{bmatrix} k+\frac{4}{3}\mu & k-\frac{2}{3}\mu & k-\frac{2}{3}\mu & 0 & 0 & 0 \\ k-\frac{2}{3}\mu & k+\frac{4}{3}\mu & k-\frac{2}{3}\mu & 0 & 0 & 0 \\ k-\frac{2}{3}\mu & k-\frac{2}{3}\mu & k+\frac{4}{3}\mu & 0 & 0 & 0 \\ 0 & 0 & 0 & 2\mu & 0 & 0 \\ 0 & 0 & 0 & 0 & 2\mu & 0 \\ 0 & 0 & 0 & 0 & 0 & 2\mu \end{bmatrix} \tag{3}$$

so that the stress-strain relation can be written in Voigt notation as $\tilde{T}=\tilde{\mathcal{C}}\tilde{\epsilon}$. We remember that instead of using the bulk modulus k and the shear modulus μ, we may adopt the Young modulus E and the Poisson ratio ν, defined in standard way

$$E=\frac{9k\mu}{\mu+3k},$$

$$\nu=\frac{3k-2\mu}{2(\mu+3k)}. \tag{4}$$

We now turn to consider the case of a solid matrix containing a single ellipsoidal void inclusion. To begin, we assume that the void has finite (and different from zero) values for its half-axes a_1, a_2, and a_3. We also suppose that the matrix is placed in an equilibrated state of uniform elastic strain $\tilde{\epsilon}^\infty$ by external loads. Accordingly, the void reaches a corresponding state of strain, which is well described by the Eshelby theory.[23,24] In particular, it is important to notice that the internal strain (i.e. inside the inclusion) is uniform if $\tilde{\epsilon}^\infty$ is so. Following the Eshelby theory, the relationship between $\tilde{\epsilon}^\infty$ and the induced internal strain $\tilde{\epsilon}^i$ is given (for voids) by[25,26]

$$\tilde{\epsilon}^i=[\tilde{I}-\tilde{\mathcal{S}}]^{-1}\tilde{\epsilon}^\infty, \tag{5}$$

where $\tilde{I}$ is the identity tensor and $\tilde{\mathcal{S}}$ is the Eshelby tensor, which depends on the aspect ratios of the ellipsoid and on the Poisson ratio ν of the matrix.[25] We consider the half-axes $a_1>a_2>a_3>0$ aligned, respectively, to the x_1, x_2, and x_3 axes of the references frame. Therefore, we define two aspect ratios as $0<e=a_3/a_2<1$ and $0<g=a_2/a_1<1$. They completely describe the shape of the void. The exact mathematical definition of the Eshelby tensor for this geometrical con-

figuration can be found in Appendix A. Further details for the ellipsoidal geometry are also reported elsewhere.[27]

Here we are interested in a flat ellipsoid (corresponding to any kind of crack) and, therefore, we must apply the above theory by considering a_3 approaching zero (or, equivalently, the aspect ratio $e \to 0$). In Eq. (5) the tensor $[\tilde{I}-\tilde{\mathcal{S}}]^{-1}$ assumes an important role: By using its matrix representation, we have developed its entries in series of the variable e. By only retaining the first order terms we get the following result[28]

$$[\tilde{I}-\tilde{\mathcal{S}}]^{-1} = \begin{bmatrix} 0 & 0 & 0 & 0 & 0 & 0 \\ 0 & 0 & 0 & 0 & 0 & 0 \\ a_{31} & a_{31} & a_{33} & 0 & 0 & 0 \\ 0 & 0 & 0 & 0 & 0 & 0 \\ 0 & 0 & 0 & 0 & a_{55} & 0 \\ 0 & 0 & 0 & 0 & 0 & a_{66} \end{bmatrix} + O(e), \quad (6)$$

where the coefficients are given below

$$a_{31} = \frac{2(1-\nu)\nu}{e(1-2\nu)\mathbf{E}},$$

$$a_{33} = \frac{2(1-\nu)^2}{e(1-2\nu)\mathbf{E}},$$

$$a_{55} = \frac{(1-\nu)(1-g^2)}{e[(1-g^2)\mathbf{E} + \nu g^2(\mathbf{E}-\mathbf{K})]},$$

$$a_{66} = \frac{(1-\nu)(1-g^2)}{e[(1-g^2)\mathbf{E} + \nu(g^2\mathbf{K}-\mathbf{E})]}. \quad (7)$$

These expressions will play a crucial role in the development of our theory. It should be understood that in Eq. (7) the argument $\sqrt{1-g^2}$ of $\mathbf{E}$ and $\mathbf{K}$ was not explicitly indicated for sake of simplicity. This abbreviation will be used throughout the paper. The functions $\mathbf{K}$ and $\mathbf{E}$ are, respectively, the complete elliptic integrals of the first kind and of the second kind, defined in Eq. (A4). For the following purposes it is also useful to introduce the quantities

$$A_{31} = \frac{2(1-\nu)\nu}{(1-2\nu)\mathbf{E}},$$

$$A_{55} = \frac{(1-\nu)(1-g^2)}{(1-g^2)\mathbf{E} + \nu g^2(\mathbf{E}-\mathbf{K})},$$

$$A_{66} = \frac{(1-\nu)(1-g^2)}{(1-g^2)\mathbf{E} + \nu(g^2\mathbf{K}-\mathbf{E})}. \quad (8)$$

Equation (8) can be used in order to rewrite Eq. (7) in the following simplified form:

$$a_{31} = \frac{A_{31}}{e},$$

$$a_{33} = \frac{(1-\nu)A_{31}}{\nu e},$$

$$a_{55} = \frac{A_{55}}{e},$$

$$a_{66} = \frac{A_{66}}{e}. \quad (9)$$

All the results of this work will be written in terms of the parameters A_{31}, A_{55}, and A_{66} depending only on the Poisson ratio ν of the solid matrix and the aspect ratio g of the cracks.

III. GENERAL THEORY FOR MULTICRACKED MATERIALS

If a given population of cracks is distributed in the solid matrix, they are typically oriented in the space with a given statistical distribution. Therefore, the first step of our procedure consists in evaluating the average value of the internal strain given in Eq. (5) over all possible orientations of the void. We label the original reference frame shown in Fig. 1 with the letter B and we name any generically rotated reference frame with the letter F. The relation between B and F is described by means of a generic rotation matrix $\hat{R}(\psi,\theta,\varphi)$ where ψ, θ and φ are the Euler angles

$$\hat{R}(\psi,\theta,\varphi) = \begin{bmatrix} \cos\psi & -\sin\psi & 0 \\ \sin\psi & \cos\psi & 0 \\ 0 & 0 & 1 \end{bmatrix} \times \begin{bmatrix} 1 & 0 & 0 \\ 0 & \cos\theta & -\sin\theta \\ 0 & \sin\theta & \cos\theta \end{bmatrix} \times \begin{bmatrix} \cos\varphi & -\sin\varphi & 0 \\ \sin\varphi & \cos\varphi & 0 \\ 0 & 0 & 1 \end{bmatrix}. \quad (10)$$

Accordingly, the following relations hold: $\hat{\epsilon}_B^i = \hat{R}\hat{\epsilon}_F^i\hat{R}^T$ for the internal strain and $\hat{\epsilon}_B^\infty = \hat{R}\hat{\epsilon}_F^\infty\hat{R}^T$ for the applied strain. These expressions can be converted into Voigt notation by defining a suitable matrix $\tilde{M}(\psi,\theta,\varphi)$, which acts as a rotation matrix on our strain vectors. We can write the change of basis as $\tilde{\epsilon}_B^i = \tilde{M}\tilde{\epsilon}_F^i$ inside the ellipsoid, and as $\tilde{\epsilon}_B^\infty = \tilde{M}\tilde{\epsilon}_F^\infty$ for the applied strain. The entries of the matrix $\tilde{M}(\psi,\theta,\varphi)$ are completely defined by direct comparison of $\hat{\epsilon}_B^i = \hat{R}\hat{\epsilon}_F^i\hat{R}^T$ with $\tilde{\epsilon}_B^i = \tilde{M}\tilde{\epsilon}_F^i$. Equation (5) written in the frame B actually reads as $\tilde{\epsilon}_B^i = [\tilde{I}-\tilde{\mathcal{S}}]^{-1}\tilde{\epsilon}_B^\infty$; it can be rotated into the generic frame F so as to give

$$\tilde{\epsilon}_F^i = \{\tilde{M}(\psi,\theta,\varphi)^{-1}[\tilde{I}-\tilde{\mathcal{S}}]^{-1}\tilde{M}(\psi,\theta,\varphi)\}\tilde{\epsilon}_F^\infty. \quad (11)$$

If we know the joint statistical distribution of the three Euler angles, we may compute the average value of the internal strain over all the corresponding rotations, weighted by the corresponding probability

$$\langle\tilde{\epsilon}_F^i\rangle = \langle\tilde{M}(\psi,\theta,\varphi)^{-1}[\tilde{I}-\tilde{\mathcal{S}}]^{-1}\tilde{M}(\psi,\theta,\varphi)\rangle\tilde{\epsilon}_F^\infty = \tilde{\mathcal{W}}\tilde{\epsilon}_F^\infty, \quad (12)$$

where the symbol $\langle\cdot\rangle$ represents the average value of the argument and $\tilde{\mathcal{W}}$ is the so-called averaged Wu tensor.[5] From now on, we will study an assembly of "effective" voids ful-

filling the relation $\langle\tilde{\epsilon}^i\rangle=\tilde{\mathcal{W}}\tilde{\epsilon}^\infty$ and distributed in the solid matrix with a given volume fraction.

We are now ready to work out the procedure aimed at defining the effective elastic behavior of a material containing cracks. We consider a volume $\mathbb{V}$ containing N voids (i.e., cracks), dispersed with an angular distribution characterized by $\tilde{\mathcal{W}}$. The volume of a single ellipsoid is $\frac{4}{3}\pi a_1 a_2 a_3 = \frac{4}{3}\pi a^3 g^2 e$, where a is the half-axis along the x_1 direction. Therefore, the volume fraction of the inclusions is given by $c=\frac{4}{3}\pi(N/\mathbb{V})a^3 g^2 e$. We may calculate the average value of the elastic strain tensor over the multicracked material by means of the relation

$$\langle\tilde{\epsilon}\rangle = c\langle\tilde{\epsilon}^i\rangle + (1-c)\tilde{\epsilon}^\infty = [(1-c)\tilde{I} + c\tilde{\mathcal{W}}]\tilde{\epsilon}^\infty, \tag{13}$$

where, assuming a small crack density, we have considered the average strain outside the inclusions similar to the bulk strain $\tilde{\epsilon}^\infty$. In this approximation (corresponding to a regime of noninteracting voids) each crack is subjected to the same external load $\tilde{\epsilon}^\infty$ and it is not affected by other neighboring cracks. We, therefore, define $\tilde{\mathcal{C}}_{\text{eff}}$ as the effective stiffness tensor of the whole anisotropic mixture by means of the relation $\langle\tilde{T}\rangle=\tilde{\mathcal{C}}_{\text{eff}}\langle\tilde{\epsilon}\rangle$. In order to evaluate $\tilde{\mathcal{C}}_{\text{eff}}$ we must calculate the average value $\langle\tilde{T}\rangle$ of the stress tensor inside the multicracked material; to this aim we must distinguish the total volume $\mathbb{V}$ of the system, the volume $\mathbb{V}_e$ of the embedded ellipsoidal voids (i.e., the cracks) and the volume $\mathbb{V}_o$ of the remaining space among the inclusions. We get

$$\begin{aligned}\langle\tilde{T}\rangle &= \frac{1}{\mathbb{V}}\int_{\mathbb{V}} \tilde{T}\,d\vec{r} = \frac{1}{\mathbb{V}}\tilde{\mathcal{C}}\int_{\mathbb{V}_o} \tilde{\epsilon}\,d\vec{r} \\ &= \frac{1}{\mathbb{V}}\tilde{\mathcal{C}}\int_{\mathbb{V}_o} \tilde{\epsilon}\,d\vec{r} + \frac{1}{\mathbb{V}}\tilde{\mathcal{C}}\int_{\mathbb{V}_e} \tilde{\epsilon}\,d\vec{r} - \frac{1}{\mathbb{V}}\tilde{\mathcal{C}}\int_{\mathbb{V}_e} \tilde{\epsilon}\,d\vec{r} \\ &= \frac{1}{\mathbb{V}}\tilde{\mathcal{C}}\int_{\mathbb{V}} \tilde{\epsilon}\,d\vec{r} - \frac{\mathbb{V}_e}{\mathbb{V}}\tilde{\mathcal{C}}\frac{1}{\mathbb{V}_e}\int_{\mathbb{V}_e} \tilde{\epsilon}\,d\vec{r} \\ &= \tilde{\mathcal{C}}\langle\tilde{\epsilon}\rangle - c\tilde{\mathcal{C}}\langle\tilde{\epsilon}^i\rangle = \tilde{\mathcal{C}}\langle\tilde{\epsilon}\rangle - c\tilde{\mathcal{C}}\tilde{\mathcal{W}}\tilde{\epsilon}^\infty.\end{aligned} \tag{14}$$

Drawing a comparison between Eqs. (13) and (14) we may find the expression for the effective stiffness tensor

$$\tilde{\mathcal{C}}_{\text{eff}} = \tilde{\mathcal{C}}\{\tilde{I} - c\tilde{\mathcal{W}}[(1-c)\tilde{I} + c\tilde{\mathcal{W}}]^{-1}\}. \tag{15}$$

Finally, in order to recover the flat shape of real cracks, we need to elaborate the above formulas in the limit of vanishing aspect ratio. Since the limit for e approaching zero is equivalent to the limit for c approaching zero, we get

$$\lim_{e\to 0} c\tilde{\mathcal{W}} = \lim_{c\to 0} c\tilde{\mathcal{W}} = \tilde{\mathcal{G}}. \tag{16}$$

where a new tensor quantity $\tilde{\mathcal{G}}$ is defined. The exact limiting value for the stiffness tensor derives from Eq. (15)

$$\tilde{\mathcal{C}}_{\text{eff}} = \tilde{\mathcal{C}}\{\tilde{I} - \tilde{\mathcal{G}}[\tilde{I} + \tilde{\mathcal{G}}]^{-1}\}, \tag{17}$$

where $\tilde{\mathcal{C}}$ is given by Eq. (3). This ends the outline of the procedure to follow for any specific statistical distribution of cracks. In the following sections we explicitly analyze two particular joint statistical distributions, leading, respectively, to the orthorhombic symmetry and to the transversely isotropic symmetry.

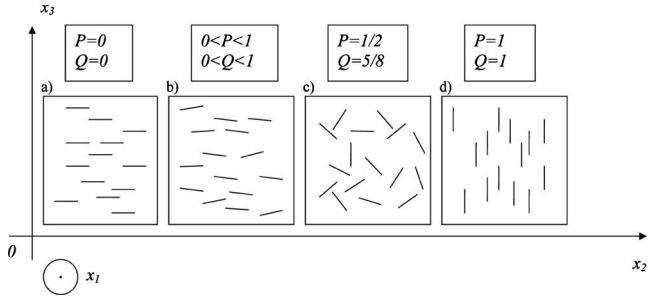

FIG. 2. Projections on the (x_2, x_3) plane of the cracks distribution in orthorhombic symmetry. The order parameters P and Q are indicated for (a), (d) the state of order and (c) disorder. Partial alignment is shown in (b).

IV. ORTHORHOMBIC SYMMETRY

A. General theory

If all the cracks (initially aligned as shown in Fig. 1) are rotated just along the x_1 axis by an angle θ, then the corresponding statistical distribution is described by a probability density $f(\theta)$ just depending on that angle θ. In other words the rotation matrix assumes the simple form

$$\hat{R}(\theta) = \begin{bmatrix} 1 & 0 & 0 \\ 0 & \cos\theta & -\sin\theta \\ 0 & \sin\theta & \cos\theta \end{bmatrix}. \tag{18}$$

In Fig. 2 one can find the projection of such a cracks distribution onto the (x_2,x_3) plane, for different probability densities $f(\theta)$. The angle θ assumes the role of a random variable, symmetrically and arbitrarily distributed over the range $(-\pi/2,\pi/2)$. For further convenience, we define the following order parameters

$$P = \langle 1-\cos^2\theta\rangle = \int_{-\pi/2}^{\pi/2} (1-\cos^2\theta) f(\theta) d\theta, \tag{19}$$

$$Q = \langle 1-\cos^4\theta\rangle = \int_{-\pi/2}^{\pi/2} (1-\cos^4\theta) f(\theta) d\theta, \tag{20}$$

which will completely describe the state of order/disorder of the orthorhombic distribution of cracks given in Fig. 2, as discussed below. It is easy to observe that if $P=Q=0$ [Fig. 2(a)], then all the cracks are parallel to the x_2 axis [horizontal order with $f(\theta)=\delta(\theta)$]; if $P=Q=1$ [Fig. 2(d)], then all the cracks are parallel to the x_3 axis [vertical order with $f(\theta)=\delta(\theta-\pi/2)$]; if $P=1/2$ and $Q=5/8$ [Fig. 2(c)], then the angle of rotation is uniformly distributed in the range $(-\pi/2,\pi/2)$, leading to a state of complete disorder [transversely isotropic medium with $f(\theta)=1/\pi$ for $-\pi/2<\theta<\pi/2$]. The remaining values [Fig. 2(b)] cover all the ori-

entational distributions between the random and the parallel ones. The average defined in Eq. (12) can be easily evaluated, getting the following expression for the Wu tensor

$$\tilde{\mathcal{W}} = \begin{bmatrix} 0 & 0 & 0 & 0 & 0 & 0 \\ \frac{A_{31}P}{e} & \frac{\beta_1}{\nu e} & \frac{\beta_2}{\nu e} & 0 & 0 & 0 \\ \frac{A_{31}(1-P)}{e} & \frac{\beta_3}{\nu e} & \frac{\beta_4}{\nu e} & 0 & 0 & 0 \\ 0 & 0 & 0 & \frac{A_{66}P}{e} & 0 & 0 \\ 0 & 0 & 0 & 0 & \frac{\beta_5}{\nu e} & 0 \\ 0 & 0 & 0 & 0 & 0 & \frac{A_{66}(1-P)}{e} \end{bmatrix}, \tag{21}$$

where the parameters β_i, $i=1,\ldots,5$, have been defined as follows:

$$\beta_1 = A_{31}[(2-3\nu)P - (1-2\nu)Q] + 2\nu A_{55}(Q-P),$$

$$\beta_2 = A_{31}[(1-2\nu)Q + (3\nu-1)P] - 2\nu A_{55}(Q-P),$$

$$\beta_3 = A_{31}[(1-2\nu)Q - (1-\nu)P + \nu] - 2\nu A_{55}(Q-P),$$

$$\beta_4 = A_{31}[(1-\nu) - \nu P - (1-2\nu)Q] + 2\nu A_{55}(Q-P),$$

$$\beta_5 = 2A_{31}(1-2\nu)(Q-P) + \nu A_{55}[1-4(Q-P)]. \tag{22}$$

The relations $\beta_1+\beta_2=A_{31}P$ and $\beta_3+\beta_4=A_{31}(1-P)$ hold and they will be useful in the following calculations. The tedious (but straightforward) calculation driving to Eq. (21) makes use of the symmetry of the probability density $f(\theta)$, which assures that the product $\sin(\theta)\cos(\theta)$ has zero average value. As a consequence, any result actually depends only on the average value of $\cos^2\theta$ and $\cos^4\theta$. This substantiates the definitions given in Eqs. (19) and (20).

By means of Eq. (16), we define the limiting value of the tensor $c\tilde{\mathcal{W}}$ for $c\to 0$, finding the tensor quantity $\tilde{\mathcal{G}}$. Through the crack density $\alpha=(a^3/V)N$, the complete structure of the tensor $\tilde{\mathcal{G}}$ is eventually found

$$\tilde{\mathcal{G}} = \frac{4}{3}\pi\alpha g^2 \times \begin{bmatrix} 0 & 0 & 0 & 0 & 0 & 0 \\ A_{31}P & \frac{\beta_1}{\nu} & \frac{\beta_2}{\nu} & 0 & 0 & 0 \\ A_{31}(1-P) & \frac{\beta_3}{\nu} & \frac{\beta_4}{\nu} & 0 & 0 & 0 \\ 0 & 0 & 0 & A_{66}P & 0 & 0 \\ 0 & 0 & 0 & 0 & \frac{\beta_5}{\nu} & 0 \\ 0 & 0 & 0 & 0 & 0 & A_{66}(1-P) \end{bmatrix}, \tag{23}$$

where the coefficients β_i have been defined in Eq. (22). It is apparent from the geometry of the multicracked material shown in Fig. 2, that its elastic behavior is different when studied along the x_1, x_2, or x_3 axis. This is proved by the calculation of the effective stiffness tensor, leading to

$$\tilde{C}_{\text{eff}} = \begin{bmatrix} C_{1111} & C_{1122} & C_{3311} & 0 & 0 & 0 \\ C_{1122} & C_{2222} & C_{2233} & 0 & 0 & 0 \\ C_{3311} & C_{2233} & C_{3333} & 0 & 0 & 0 \\ 0 & 0 & 0 & C_{1212} & 0 & 0 \\ 0 & 0 & 0 & 0 & C_{2323} & 0 \\ 0 & 0 & 0 & 0 & 0 & C_{3131} \end{bmatrix} \tag{24}$$

corresponding to a solid with orthorhombic symmetry, described by nine independent elastic moduli. A straightforward application of Eq. (17) drives to obtain the following expressions for the stiffness tensor entries

$$C_{1111} = \frac{E}{D}\left[(1-\nu) + \frac{4\pi\alpha g^2}{3}\frac{(\beta_1+\beta_4)(1-\nu) - A_{31}\nu^2}{\nu} + \frac{16}{9}\pi^2\alpha^2 g^4(1+\nu)(1-2\nu)A_{31}\frac{\beta_1(1-P)-\beta_3 P}{\nu^2}\right],$$

$$C_{2222} = \frac{E}{D}\left[(1-\nu) + \frac{4}{3}\pi\alpha g^2\frac{\beta_4(1-\nu)-\beta_3\nu}{\nu}\right],$$

$$C_{3333} = \frac{E}{D}\left[(1-\nu) + \frac{4}{3}\pi\alpha g^2\frac{\beta_1(1-\nu)-\beta_2\nu}{\nu}\right],$$

$$C_{1122} = \nu\frac{E}{D}\left[1 + \frac{4}{3}\pi\alpha g^2\frac{\beta_4-\beta_3}{\nu}\right],$$

$$C_{2233} = \nu\frac{E}{D}\left[1 + \frac{4}{3}\pi\alpha g^2\frac{\beta_1\nu-\beta_2(1-\nu)}{\nu^2}\right],$$

$$C_{3311} = \nu\frac{E}{D}\left[1 + \frac{4}{3}\pi\alpha g^2\frac{\beta_1-\beta_2}{\nu}\right],$$

$$C_{1212} = \frac{E}{(1+\nu)\left[1+\frac{4}{3}\pi\alpha g^2 A_{66} P\right]},$$

$$C_{2323} = \frac{E}{(1+\nu)\left[1+\frac{4}{3}\pi\alpha g^2 \frac{\beta_5}{\nu}\right]},$$

$$C_{3131} = \frac{E}{(1+\nu)\left[1+\frac{4}{3}\pi\alpha g^2 A_{66}(1-P)\right]}, \tag{25}$$

where we have used the definition

$$D = (1+\nu)(1-2\nu)\times\left[1+\frac{4}{3}\pi\alpha g^2\frac{\beta_1+\beta_4}{\nu} + \frac{16}{9}\pi^2\alpha^2 g^4\frac{\beta_1\beta_4-\beta_2\beta_3}{\nu^2}\right]. \tag{26}$$

Equation (25) represents the complete elastic characterization of a solid with a given orthorhombic distribution of elliptic cracks, under the hypothesis of small crack density. It is important to underline that the overall stiffness tensor of the solid depends on the orientational distribution $f(\theta)$ only through the two averages P and Q.

Equation (25) can be specified for a particular case relevant for the applications: we can in fact obtain a distribution of slit-cracks by performing the limit $a_1 \to \infty$ (or, equivalently, $g \to 0$ since $a_2 = g a_1$). In this case we may define a two-dimensional version for the crack density as $\gamma = \pi a_2^2 (N/A)$, where we have considered N slit-cracks distributed over the area A of the (x_2, x_3) plane (a_2 is the half-length of the Griffith crack). Since the volume fraction can be now written as $c = \frac{4}{3}\pi\alpha g^2 e = \gamma e$, we obtain the simple relation $\alpha = \frac{3}{4}(\gamma/\pi g^2)$. By using such a relation in Eq. (25) and performing the limit of $g \to 0$, we obtain the following result

$$C_{1111} = \frac{[4\gamma^2 P(1-P)(1-\nu^2)+2\gamma+1](1-\nu)E}{[4\gamma^2 P(1-P)(1-\nu)^2+2(1-\nu)^2\gamma+1-2\nu](1+\nu)},$$

$$C_{2222} = \frac{(1-\nu)[1+2(1-P)\gamma]E}{[4\gamma^2 P(1-P)(1-\nu)^2+2(1-\nu)^2\gamma+1-2\nu](1+\nu)},$$

$$C_{3333} = \frac{(1-\nu)[1+2\gamma P]E}{[4\gamma^2 P(1-P)(1-\nu)^2+2(1-\nu)^2\gamma+1-2\nu](1+\nu)},$$

$$C_{1122} = \frac{\nu[1+2(1-P)(1-\nu)\gamma]E}{[4\gamma^2 P(1-P)(1-\nu)^2+2(1-\nu)^2\gamma+1-2\nu](1+\nu)},$$

$$C_{2233} = \frac{\nu E}{[4\gamma^2 P(1-P)(1-\nu)^2+2(1-\nu)^2\gamma+1-2\nu](1+\nu)},$$

$$C_{3311} = \frac{\nu[1+2P(1-\nu)\gamma]E}{[4\gamma^2 P(1-P)(1-\nu)^2+2(1-\nu)^2\gamma+1-2\nu](1+\nu)},$$

$$C_{1212} = \frac{E}{(1+\gamma P)(1+\nu)},$$

$$C_{2323} = \frac{E}{[1+(1-\nu)\gamma](1+\nu)},$$

$$C_{3131} = \frac{E}{[1+\gamma(1-P)](1+\nu)}. \tag{27}$$

These relations are in agreement with those described in recent works,[16,17] which therefore represent a special case of the present general theory. It is interesting to observe that when dealing with slit-cracks, the effects of the order parameter Q completely vanish, the final results being dependent only on P [see Eq. (27)].

We now return to the more general case of elliptic cracks. When they are uniformly oriented in the (x_2, x_3) plane, the overall multicracked material is transversely isotropic and the order parameters assume the value $P = 1/2$ and $Q = 5/8$, then the corresponding stiffness tensor given by Eq. (24) is

$$\tilde{C}_{\text{eff}} = \begin{bmatrix} n & l & l & 0 & 0 & 0 \\ l & k+m & k-m & 0 & 0 & 0 \\ l & k-m & k+m & 0 & 0 & 0 \\ 0 & 0 & 0 & 2p & 0 & 0 \\ 0 & 0 & 0 & 0 & 2m & 0 \\ 0 & 0 & 0 & 0 & 0 & 2p \end{bmatrix}, \tag{28}$$

where the five Hill parameters (typically used for transverse isotropy as described in Ref. 10) can be calculated from Eq. (25)

$$n = E\frac{1-\nu}{1+\nu}\frac{1+\frac{4}{3}\pi\alpha g^2\frac{1+\nu}{\mathbf{E}}}{1-2\nu+\frac{4}{3}\pi\alpha g^2\frac{1-\nu}{\mathbf{E}}},$$

$$l = E\frac{\nu}{1+\nu}\frac{1}{1-2\nu+\frac{4}{3}\pi\alpha g^2\frac{1-\nu}{\mathbf{E}}},$$

$$k = E\frac{1}{2(1+\nu)}\frac{1}{1-2\nu+\frac{4}{3}\pi\alpha g^2\frac{1-\nu}{\mathbf{E}}},$$

$$m = E\frac{1}{2(1+\nu)}\frac{1}{1+\frac{2}{3}\pi\alpha g^2\frac{1-\nu}{\mathbf{E}}\frac{2(1-g^2)\mathbf{E}+\nu g^2(\mathbf{E}-\mathbf{K})}{(1-g^2)\mathbf{E}+\nu g^2(\mathbf{E}-\mathbf{K})}},$$

$$p = E\frac{1}{2(1+\nu)}\frac{1}{1+\frac{2}{3}\pi\alpha g^2\frac{(1-g^2)(1-\nu)}{(1-g^2)\mathbf{E}+\nu(g^2\mathbf{K}-\mathbf{E})}}. \tag{29}$$

The argument $\sqrt{1-g^2}$ of the elliptic integrals is once again omitted for sake of brevity. As before, we may consider the

particular case of a distribution of slit-cracks: By using the previous relation $\alpha=\frac{3}{4}(\gamma/\pi g^2)$ in Eq. (29), we perform the limit for $g\to 0$ of the Hill parameters, obtaining

$$n=\frac{[1+\gamma(1+\nu)](1-\nu)}{[1-2\nu+(1-\nu)\gamma](1+\nu)}E,$$

$$l=\frac{\nu}{[1-2\nu+(1-\nu)\gamma](1+\nu)}E,$$

$$k=\frac{1}{2[1-2\nu+(1-\nu)\gamma](1+\nu)}E,$$

$$m=\frac{1}{2[1+(1-\nu)\gamma](1+\nu)}E,$$

$$p=\frac{1}{(2+\gamma)(1+\nu)}E. \tag{30}$$

This result corresponds to our previous investigations.[16,17] However, we remark that it is obtained here as a special case of a much more general theory.

B. Two-dimensional elasticity

Typically, in two-dimensional (2D) elasticity a transversely isotropic medium can be loaded under plane stress or plane strain conditions. In this section we analyze the 2D elastic behavior of a body described by a stiffness tensor as in Eqs. (28) and (29) in both conditions.

We begin with the hypothesis of plane stress [on the (x_2,x_3) plane]: It is easy to prove that a transversely isotropic material corresponds to an isotropic one with effective Young modulus and Poisson ratio given by

$$E_{\text{eff}}=\frac{4m(l^2-nk)}{l^2-nk-nm},$$

$$\nu_{\text{eff}}=\frac{l^2-nk+nm}{l^2-nk-nm}. \tag{31}$$

In addition, by using Eq. (31) with the Hill parameters defined in Eq. (29), we obtain the effective elastic moduli in the form of first order expansions in the parameter α

$$E_{\text{eff}}=E\left[1-\pi\alpha g^2(1-\nu^2)\frac{\frac{4}{3}(1-g^2)\mathbf{E}+\nu g^2(\mathbf{E}-\mathbf{K})}{\mathbf{E}[(1-g^2)\mathbf{E}+\nu g^2(\mathbf{E}-\mathbf{K})]}\right], \tag{32}$$

$$\nu_{\text{eff}}=\nu\left[1-\pi\alpha g^2(1-\nu^2)\times\frac{\frac{1}{3}(\mathbf{E}-g^2\mathbf{K})+(1-g^2)\mathbf{E}+\nu g^2(\mathbf{E}-\mathbf{K})}{\mathbf{E}[(1-g^2)\mathbf{E}+\nu g^2(\mathbf{E}-\mathbf{K})]}\right]. \tag{33}$$

We remark that the above equations are valid only for small crack density.

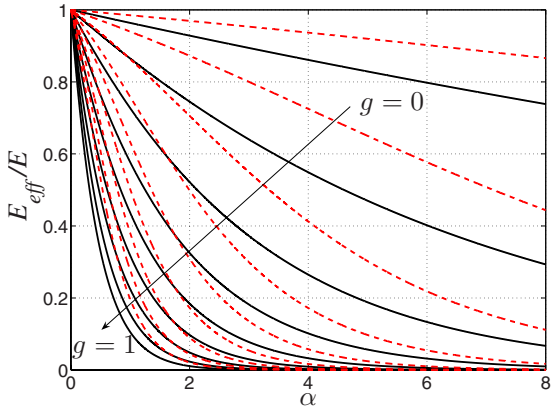

FIG. 3. (Color online) Effective Young modulus E_{eff} vs the crack density α under plane stress condition. The continuous lines correspond to the positive matrix Poisson ratio $\nu=0.33$, while the dashed lines correspond to the negative matrix Poisson ratio $\nu=-0.8$. The aspect ratio g ranges from 0.1 to 0.9.

Equations (32) and (33) are very useful to exploit the iterated homogenization method, that allows us to generalize our results to large crack density values. Let us suppose that the effective moduli of a multicracked medium (containing an initial number N of cracks) are known to be $E_{\text{eff}}(N)$ and $\nu_{\text{eff}}(N)$. If a small additional number ΔN of cracks is added to the matrix, then the change in the elastic moduli is approximately the same as if they were added to a uniform and homogeneous matrix with moduli $E_{\text{eff}}(N)$ and $\nu_{\text{eff}}(N)$. The resulting elastic moduli will be therefore $E_{\text{eff}}(N+\Delta N)$ and $\nu_{\text{eff}}(N+\Delta N)$, as obtained by Eqs. (32) and (33), through the replacements: $E\to E_{\text{eff}}(N)$, $\nu\to\nu_{\text{eff}}(N)$, $E_{\text{eff}}\to E_{\text{eff}}(N+\Delta N)$, $\nu_{\text{eff}}\to\nu_{\text{eff}}(N+\Delta N)$ and $\alpha=(a^3/V)\Delta N$. We obtain a set of difference equations that, in the limit of vanishingly small ΔN, converges to a couple of differential equations

$$\frac{dE_{\text{eff}}}{dN}=-E_{\text{eff}}\pi\frac{a^3}{V}g^2(1-\nu_{\text{eff}}^2)\times\frac{\frac{4}{3}(1-g^2)\mathbf{E}+\nu_{\text{eff}}g^2(\mathbf{E}-\mathbf{K})}{\mathbf{E}[(1-g^2)\mathbf{E}+\nu_{\text{eff}}g^2(\mathbf{E}-\mathbf{K})]}, \tag{34}$$

$$\frac{d\nu_{\text{eff}}}{dN}=-\nu_{\text{eff}}\pi\frac{a^3}{V}g^2(1-\nu_{\text{eff}}^2)\times\frac{\frac{1}{3}(\mathbf{E}-g^2\mathbf{K})+(1-g^2)\mathbf{E}+\nu_{\text{eff}}g^2(\mathbf{E}-\mathbf{K})}{\mathbf{E}[(1-g^2)\mathbf{E}+\nu_{\text{eff}}g^2(\mathbf{E}-\mathbf{K})]}. \tag{35}$$

This procedure is commonly referred to as differential effective medium theory.[11] The differential system given in Eqs. (34) and (35) is separable and it can be analytically solved by means of the integration of rational functions. The complete expressions are not reported here for brevity, but it is interesting to observe that the solutions depend exponentially on the crack density α. This fact explains the strong and rapid damaging of a medium containing an increasing number of cracks in a given region.[20] In Fig. 3 and Fig. 4 the solutions of Eqs. (34) and (35) are represented both for positive and

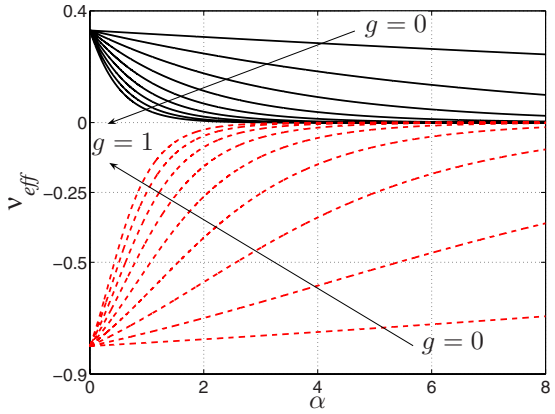

FIG. 4. (Color online) Effective Poisson ratio ν_{eff} vs the crack density α under plane stress condition. The continuous lines correspond to the positive matrix Poisson ratio ν=0.33, while the dashed lines correspond to the negative matrix Poisson ratio ν=−0.8. The aspect ratio g ranges from 0.1 to 0.9.

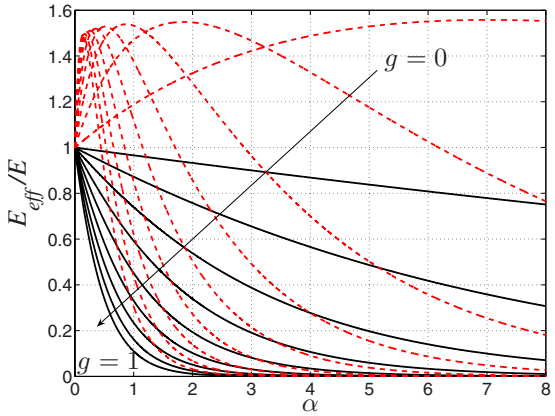

FIG. 5. (Color online) Effective Young modulus E_{eff} vs the crack density α under plane strain condition. The continuous lines correspond to the positive matrix Poisson ratio ν=0.33, while the dashed lines correspond to the negative matrix Poisson ratio ν =−0.8. The aspect ratio g ranges from 0.1 to 0.9.

negative values of the matrix Poisson ratio and for different aspect ratios g of the elliptic cracks. Under plane stress condition, the Young modulus and the Poisson ratio of the multicracked material decrease to zero more slowly if the matrix Poisson ratio is negative.

Let us now turn to the plane strain case. Under this border condition it is simple to verify that the transversely isotropic material, defined by Eq. (28), corresponds to an isotropic one with Young modulus and Poisson ratio given by

$$E_{\text{eff}} = \frac{m}{k}(3k - m),$$

$$\nu_{\text{eff}} = \frac{k - m}{2k}. \tag{36}$$

Moreover, by using Eq. (36) with the Hill parameters defined in Eq. (29), we obtain the first order expansions in the parameter α of the effective elastic moduli

$$E_{\text{eff}} = E\left[1 - \pi\alpha g^2 \frac{1-\nu}{1+\nu} \times \frac{\frac{4+5\nu}{3}(1-g^2)\mathbf{E} + \frac{4}{3}\nu^2 g^2(\mathbf{E}-\mathbf{K}) + \nu(\mathbf{E}-g^2\mathbf{K})}{\mathbf{E}[(1-g^2)\mathbf{E} + \nu g^2(\mathbf{E}-\mathbf{K})]}\right], \tag{37}$$

$$\nu_{\text{eff}} = \nu\left[1 - \pi\alpha g^2(1-\nu) \times \frac{\frac{1}{3}(\mathbf{E}-g^2\mathbf{K}) + (1-g^2)\mathbf{E} + \frac{2}{3}\nu g^2(\mathbf{E}-\mathbf{K})}{\mathbf{E}[(1-g^2)\mathbf{E} + \nu g^2(\mathbf{E}-\mathbf{K})]}\right]. \tag{38}$$

As before, knowledge of the first order expansions is useful to apply to the iterated homogenization method, leading to the following system of differential equations

$$\frac{dE_{\text{eff}}}{dN} = -E_{\text{eff}}\pi\frac{a^3}{V}g^2\frac{1-\nu_{\text{eff}}}{1+\nu_{\text{eff}}} \times \frac{\frac{4+5\nu_{\text{eff}}}{3}(1-g^2)\mathbf{E} + \frac{4}{3}\nu_{\text{eff}}^2 g^2(\mathbf{E}-\mathbf{K}) + \nu_{\text{eff}}(\mathbf{E}-g^2\mathbf{K})}{\mathbf{E}[(1-g^2)\mathbf{E} + \nu_{\text{eff}} g^2(\mathbf{E}-\mathbf{K})]}, \tag{39}$$

$$\frac{d\nu_{\text{eff}}}{dN} = -\nu_{\text{eff}}\pi\frac{a^3}{V}g^2(1-\nu_{\text{eff}}) \times \frac{\frac{1}{3}(\mathbf{E}-g^2\mathbf{K}) + (1-g^2)\mathbf{E} + \frac{2}{3}\nu_{\text{eff}} g^2(\mathbf{E}-\mathbf{K})}{\mathbf{E}[(1-g^2)\mathbf{E} + \nu_{\text{eff}} g^2(\mathbf{E}-\mathbf{K})]}. \tag{40}$$

Once again, the analytical solutions provide an exponential dependence upon the crack density α. They are not reported here, but in Fig. 5 and Fig. 6 one can find the trend of the effective elastic moduli obtained by the numerical solution of Eqs. (39) and (40).

An interesting unconventional behavior of the effective Young modulus of the multicracked solid is observed in Fig. 5 for a negative matrix Poisson ratio. When $-1 < \nu < -1/2$ we obtain an effective Young modulus greater than the Young modulus of the original elastic matrix for low values of α. This effect is shown in Fig. 5 where a value ν=−0.8 is assumed. Our choice corresponds to the realistic case reported for foams.[29] This effect is not present under plane stress conditions. This unusual behavior can be attributed to the specific meaning of the Young modulus in plane strain condition: The elastically loaded plain strain system has fewer degrees of freedom than the system in plane stress, because of the peculiar boundary conditions needed to avoid the appearing of out-of-plane strain in the solid. This means that, when one measures the Young modulus on a given direction in plane strain conditions, some other forces must be applied in the orthogonal directions in order to fulfill the plain strain state, generating a very special set of loading.

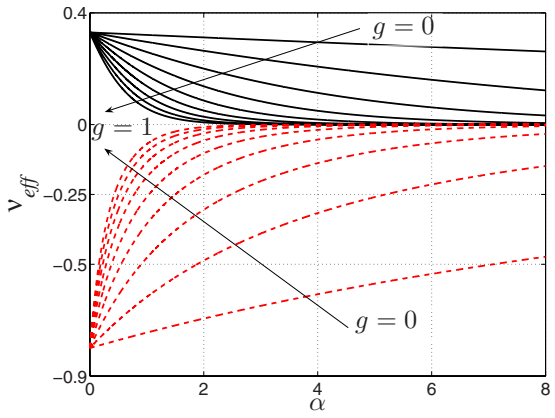

FIG. 6. (Color online) Effective Poisson ratio ν_{eff} vs the crack density α under plane strain condition. The continuous lines correspond to the positive matrix Poisson ratio ν=0.33, while the dashed lines correspond to the negative matrix Poisson ratio ν=−0.8. The aspect ratio g ranges from 0.1 to 0.9.

In conclusion, for a negative Poisson ratio, a fractured medium can be stiffer than the original matrix, contrary to common expectations. This phenomenon has been observed also in the particular case of slit cracks ($g \to 0$), as recently reported.[16]

V. TRANSVERSELY ISOTROPIC SYMMETRY

A. General theory

In this section we are dealing with a different distribution of elliptic cracks in isotropic solids. We consider a given orthonormal reference frame and we take the x_3 axis as preferential direction of alignment. The overall medium has a positional disorder, but a partial orientational order and it exhibits a uniaxial behavior: The situation is shown in Fig. 7. The normal direction of each crack forms an angle θ with the x_3 axis; the angular distribution is described by a probability density $f(\theta)$, defined in $[0\ \pi]$. Moreover, each elliptic crack can be randomly rotated around its normal direction. The orientation of each crack is statistically independent from the orientation of the other ones. If $f(\theta)=\delta(\theta)$ we have all the cracks with θ=0 and, therefore, their normal vectors are

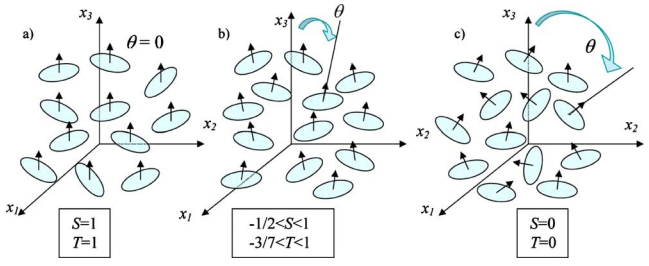

FIG. 7. (Color online) Transversely isotropic structure of a multicracked solid with elliptic cracks in three-dimensional elasticity. The order parameters S and T are indicated for (a) the state of order and (c) the state of disorder. An intermediate configuration is shown in (b).

all oriented along the x_3 axis [see Fig. 7(a)]. If $f(\theta)=(1/2)\sin(\theta)$, then all the cracks are uniformly random oriented in the space over all the possible orientations [see Fig. 7(c)]. Any other statistical distribution $f(\theta)$ defines a transversely isotropic (uniaxial) material [see Fig. 7(b)].

Referring to the Euler angles ψ, θ, and φ described in Sec. III, we evaluate at first the average value of the strain inside the inclusion over the angles φ and ψ (which are uniformly distributed over the range $[0\ 2\pi]$). Then, we perform a second averaging over the remaining angle θ described by the above probability density $f(\theta)$. We get

$$\langle \tilde{\epsilon}^i \rangle = \frac{1}{4\pi^2}\int_0^{2\pi}\int_0^{2\pi}\int_0^{\pi} \tilde{M}^{-1}[\tilde{I}-\tilde{S}]^{-1}\tilde{M} f(\theta)\, d\theta\, d\varphi\, d\psi\, \tilde{\epsilon}^{\infty} = \tilde{\mathcal{W}}\tilde{\epsilon}^{\infty}. \tag{41}$$

A tedious integration leads to the following general structure for the Wu tensor

$$\tilde{\mathcal{W}} = \begin{bmatrix} \mathcal{W}_{11} & \mathcal{W}_{12} & \mathcal{W}_{13} & 0 & 0 & 0 \\ \mathcal{W}_{12} & \mathcal{W}_{11} & \mathcal{W}_{13} & 0 & 0 & 0 \\ \mathcal{W}_{31} & \mathcal{W}_{31} & \mathcal{W}_{33} & 0 & 0 & 0 \\ 0 & 0 & 0 & \mathcal{W}_{11}-\mathcal{W}_{12} & 0 & 0 \\ 0 & 0 & 0 & 0 & \mathcal{W}_{55} & 0 \\ 0 & 0 & 0 & 0 & 0 & \mathcal{W}_{55} \end{bmatrix} \tag{42}$$

and the corresponding entries are

$$\mathcal{W}_{11} = \left(\frac{2}{15} - \frac{3}{35}T - \frac{1}{21}S\right)(a_{31}+a_{55}+a_{66}) + \left(\frac{3}{35}T - \frac{2}{7}S + \frac{1}{5}\right)a_{33},$$

$$\mathcal{W}_{12} = \left(\frac{2}{21}S - \frac{1}{15} - \frac{1}{35}T\right)(a_{55}+a_{66}-a_{33}) + \left(\frac{4}{15} - \frac{1}{35}T - \frac{5}{21}S\right)a_{31},$$

$$\mathcal{W}_{13} = \left(\frac{4}{35}T - \frac{1}{21}S - \frac{1}{15}\right)(a_{55}+a_{66}-a_{33}) + \left(\frac{4}{15} - \frac{8}{21}S + \frac{4}{35}T\right)a_{31},$$

$$\mathcal{W}_{31} = \left(\frac{4}{35}T - \frac{1}{21}S - \frac{1}{15}\right)(a_{55}+a_{66}-a_{33}) + \left(\frac{4}{35}T + \frac{13}{21}S + \frac{4}{15}\right)a_{31},$$

$$\mathcal{W}_{33} = \left(\frac{2}{15} - \frac{8}{35}T + \frac{2}{21}S\right)(a_{31} + a_{55} + a_{66}) + \left(\frac{8}{35}T + \frac{4}{7}S + \frac{1}{5}\right)a_{33},$$

$$\mathcal{W}_{55} = \left(\frac{1}{14}S + \frac{8}{35}T + \frac{1}{5}\right)(a_{55} + a_{66}) + \left(\frac{2}{21}S + \frac{2}{15} - \frac{8}{35}T\right)(a_{33} - a_{31}), \tag{43}$$

where a_{31}, a_{33}, a_{55} and a_{66} are defined in Eq. (7). We want to point out that these expressions are extremely useful to perform the averaging procedure, since they remove the problem of the integral evaluation and provide results in a closed form.

The elastic moduli of the material depend on the state of order through the parameters $S=\langle P_2(\cos\theta)\rangle$ and $T=\langle P_4(\cos\theta)\rangle$. They correspond to the average values of the Legendre polynomial of order two and four, respectively, computed by means of the probability density $f(\theta)$

$$S = \int_0^\pi \left(\frac{3}{2}\cos^2\theta - \frac{1}{2}\right) f(\theta) d\theta, \tag{44}$$

$$T = \int_0^\pi \left(\frac{35}{8}\cos^4\theta - \frac{15}{4}\cos^2\theta + \frac{3}{8}\right) f(\theta) d\theta. \tag{45}$$

This two order parameters fulfill the following bounds: $-1/2 < S < 1$ and $-3/7 < T < 1$. Three particular cases can be taken into consideration: If $S=T=1$, then the system lies in a state of order (cracks have the normal unit vectors aligned to the x_3 axis); if $S=T=0$, then the system is fully disordered (cracks are randomly oriented); finally, if $S=-1/2$ and $T=3/8$, then all crack normal unit vectors are lying randomly in planes perpendicular to the x_3 axis. Following the same procedure outlined in the previous sections, we determine the general expression of the effective stiffness tensor (a list of the entries of $\widetilde{\mathcal{G}}$ is given in Appendix B)

$$\widetilde{\mathcal{C}}_{\text{eff}} = \begin{bmatrix} k+m & k-m & l & 0 & 0 & 0 \\ k-m & k+m & l & 0 & 0 & 0 \\ l & l & n & 0 & 0 & 0 \\ 0 & 0 & 0 & 2m & 0 & 0 \\ 0 & 0 & 0 & 0 & 2p & 0 \\ 0 & 0 & 0 & 0 & 0 & 2p \end{bmatrix}. \tag{46}$$

The complete expressions of the corresponding Hill parameters are very complicated and, above all, they are not very useful to better understanding the physics of the multicracking process. We therefore do not report them. Rather, we believe that it is worthy to show their series expansions up to the first order in the crack density α

$$n = \frac{E(1-\nu)}{(1-2\nu)(1+\nu)} - \frac{4}{45}E\pi g^2 \frac{A_{31}(3-2\nu+7\nu^2) + 2(A_{66}+A_{55})\nu(1-2\nu)}{\nu(1-2\nu)(1+\nu)}\alpha - \frac{8}{63}E\pi g^2 \frac{2A_{31}(3+\nu) + (A_{66}+A_{55})\nu}{\nu(1+\nu)}\alpha S + \frac{32}{105}E\pi g^2 \frac{(A_{66}+A_{55})\nu - A_{31}(1-2\nu)}{\nu(1+\nu)}\alpha T, \tag{47}$$

$$l = \frac{E\nu}{(1-2\nu)(1+\nu)} - \frac{4}{45}E\pi g^2 \frac{A_{31}(1+6\nu-\nu^2) - (A_{66}+A_{55})\nu(1-2\nu)}{\nu(1-2\nu)(1+\nu)}\alpha - \frac{4}{63}E\pi g^2 \frac{A_{31}(1+5\nu) - (A_{66}+A_{55})\nu}{\nu(1+\nu)}\alpha S - \frac{16}{105}E\pi g^2 \frac{(A_{66}+A_{55})\nu - A_{31}(1-2\nu)}{\nu(1+\nu)}\alpha T, \tag{48}$$

$$k = \frac{E(1-\nu)}{(1-2\nu)(1+\nu)} - \frac{2}{45}E\pi g^2 \frac{2A_{31}(2+2\nu+3\nu^2) + (A_{66}+A_{55})\nu(1-2\nu)}{\nu(1-2\nu)(1+\nu)}\alpha + \frac{2}{63}E\pi g^2 \frac{4A_{31}(2+3\nu) - (A_{66}+A_{55})\nu}{\nu(1+\nu)}\alpha S + \frac{8}{105}E\pi g^2 \frac{(A_{66}+A_{55})\nu - A_{31}(1-2\nu)}{\nu(1+\nu)}\alpha T, \tag{49}$$

$$m = \frac{E}{2(1+\nu)} - \frac{2}{45}E\pi g^2 \frac{2A_{31}(1-2\nu) + 3(A_{66}+A_{55})\nu}{\nu(1+\nu)}\alpha + \frac{2}{63}E\pi g^2 \frac{4A_{31}(1-2\nu) + 3(A_{66}+A_{55})\nu}{\nu(1+\nu)}\alpha S + \frac{4}{105}E\pi g^2 \frac{(A_{66}+A_{55})\nu - A_{31}(1-2\nu)}{\nu(1+\nu)}\alpha T, \tag{50}$$

$$p = \frac{E}{2(1+\nu)} - \frac{2}{45}E\pi g^2 \frac{2A_{31}(1-2\nu) + 3(A_{66}+A_{55})\nu}{\nu(1+\nu)}\alpha - \frac{1}{63}E\pi g^2 \frac{4A_{31}(1-2\nu) + 3(A_{66}+A_{55})\nu}{\nu(1+\nu)}\alpha S + \frac{16}{105}E\pi g^2 \frac{A_{31}(1-2\nu) - (A_{66}+A_{55})\nu}{\nu(1+\nu)}\alpha T. \tag{51}$$

In each of these expressions the terms have been ordered with the following rule: The first term represents the Hill modulus for an isotropic solid without cracks; the second term represents the perturbation due to isotropic cracking

($S=T=0$) of the material; and the last two terms represent two additional perturbations, taking into account the particular angular distribution described by S and T. Approximated expressions given in Eqs. (47)–(51) hold only for a small crack density. Of course, the exact procedure can be numerically implemented by means of Eq. (17) and the expressions listed in Appendix B.

B. Results and discussion

In order to obtain practical results, it is a common choice[30] to introduce a specific probability density, bridging the random and the parallel orientations through a single coefficient. By following this method, we need to guess a probability density depending on a coefficient χ (varying from $-\infty$ to $+\infty$) and, accordingly, to calculate the order parameters S and T. When $\chi \to -\infty$, a state of order is found, where all the cracks (actually, their normal vectors) are aligned with the x_3 axis; on the other hand, when $\chi=0$, a state of disorder is represented, where all the cracks are uniformly random oriented in the space; finally, when $\chi \to +\infty$, the crack normal vectors are orthogonal to the x_3 axis. A possible expression of the normalized probability density fulfilling the above conditions is

$$f(\theta) = \begin{cases} \frac{1}{2}\sin(\theta)\frac{(\chi^2+1)e^{\chi\theta}}{\chi e^{(\pi/2)\chi}+1} & \text{if } 0 < \theta < \frac{\pi}{2}, \\ \frac{1}{2}\sin(\theta)\frac{(\chi^2+1)e^{\chi(\pi-\theta)}}{\chi e^{(\pi/2)\chi}+1} & \text{if } \frac{\pi}{2} < \theta < \pi. \end{cases} \tag{52}$$

The average values of $\cos^2\theta$ and $\cos^4\theta$, appearing in Eq. (44) and Eq. (45), can be easily calculated[31]

$$C_2 = \int_0^{\pi} \cos^2\theta f(\theta) d\theta = \frac{2\chi e^{(\pi/2)\chi} + \chi^2 + 3}{(\chi^2+9)(\chi e^{(\pi/2)\chi}+1)}, \tag{53}$$

$$C_4 = \int_0^{\pi} \cos^4\theta f(\theta) d\theta = \frac{24\chi e^{(\pi/2)\chi} + \chi^4 + 22\chi^2 + 45}{(\chi^2+25)(\chi^2+9)(\chi e^{(\pi/2)\chi}+1)}. \tag{54}$$

From Eq. (44) and Eq. (45) we immediately obtain the order parameters

$$S = \frac{3}{2}C_2 - \frac{1}{2}, \tag{55}$$

$$T = \frac{35}{8}C_4 - \frac{15}{4}C_2 + \frac{3}{8}. \tag{56}$$

Eventually, we may compute the effective Hill parameters of the multicracked material in terms of the quantity χ, the aspect ratio g, the matrix moduli E and ν, and the crack density α. They are reported in Fig. 8 (in arbitrary units) versus χ and g. We have considered a model system corresponding to an isotropic matrix with $E=1$ (a.u.) and $\nu=0.35$ and a fixed crack density $\alpha=5$. It is interesting to observe that the five Hill parameters have a different qualitative behavior versus the coefficient χ. More precisely, we can say that the parameters k and m are monotonically decreasing [see Figs. 8(a) and 8(c), dotted lines] and parameters n and p are monotonically increasing [see Figs. 8(a) and 8(c), continuous lines] versus the state of order/disorder. Moreover, the Hill parameter l is unimodal [see Fig. 8(b), dotted lines], i.e., it is monotonically decreasing up to $\chi \approx 0$ and then monotonically increasing.

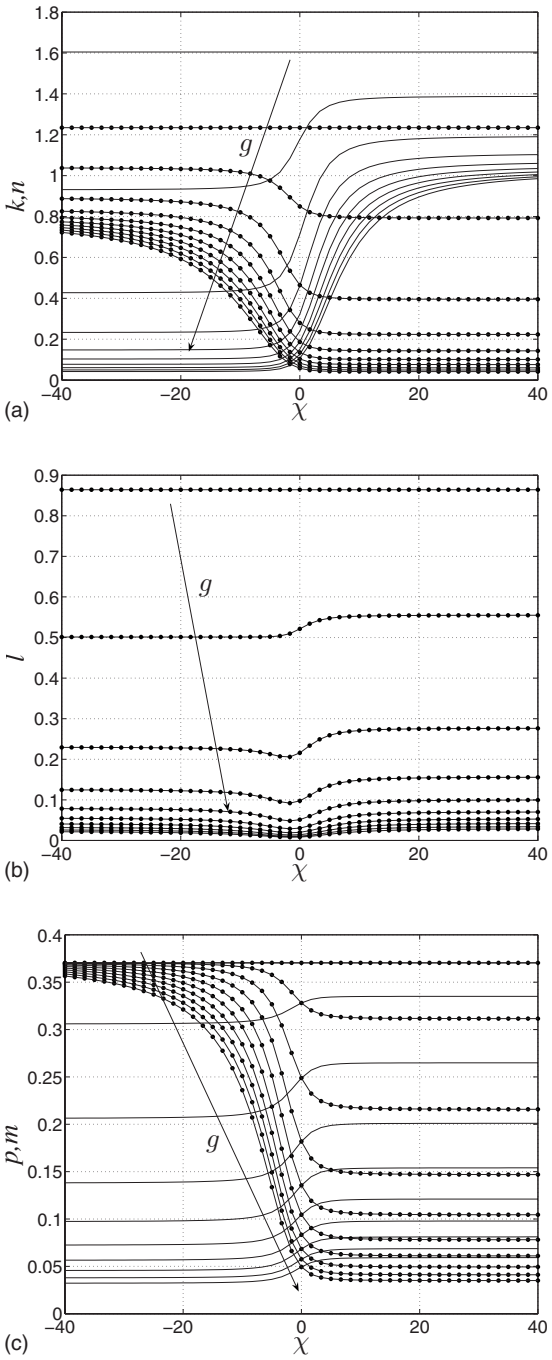

FIG. 8. Effective Hill parameters of the multicracked material vs the coefficient χ. (a) k (dotted lines) and n (continuous lines). (b) l (dotted lines). (c) m (dotted lines) and p (continuous lines). The aspect ratio g ranges from 0 to 1. We have set $E=1$, $\nu=0.35$, and $\alpha=5$ (arbitrary units).

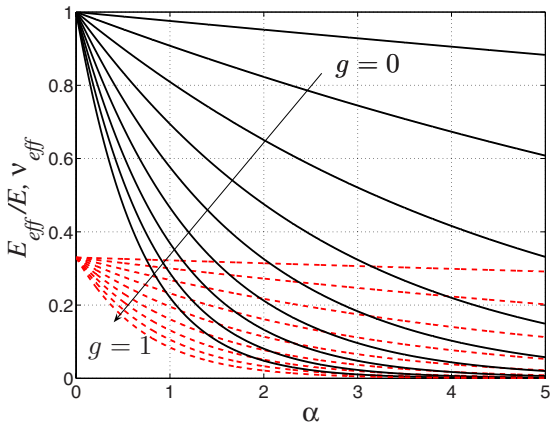

FIG. 9. (Color online) Effective moduli E_{eff} (continuous lines) and ν_{eff} (dashed lines) vs the crack density α for a 3D isotropic distribution of cracks. The aspect ratio g ranges from 0.1 to 0.9. We have set $\nu=0.33$.

C. Three-dimensional isotropic distribution of cracks

When the distribution of elliptic cracks is completely random in 3D, we can use the values $S=T=0$ in Eqs. (47)–(51) and we obtain an overall isotropic behavior of the multicracked medium. It is described by an effective Young modulus and an effective Poisson ratio [see Fig. 7(c)]. In order to cope with large values of the crack density, we can adopt the differential scheme (see Sec. IV B), obtaining

$$\frac{dE_{\text{eff}}}{dN} = -E_{\text{eff}}\frac{8\pi a^3}{15V}g^2(1-\nu_{\text{eff}}^2) \times\left[\frac{1}{\mathbf{E}}+\frac{1}{3}\frac{1-g^2}{(1-g^2)\mathbf{E}+\nu_{\text{eff}}g^2(\mathbf{E}-\mathbf{K})} +\frac{1}{3}\frac{1-g^2}{(1-g^2)\mathbf{E}+\nu_{\text{eff}}(g^2\mathbf{K}-\mathbf{E})}\right], \tag{57}$$

$$\frac{d\nu_{\text{eff}}}{dN} = -\frac{8\pi a^3}{45V}g^2(1-\nu_{\text{eff}}^2) \times\left[\frac{1+3\nu_{\text{eff}}}{\mathbf{E}}-\frac{1}{2}\frac{(1-g^2)(1-2\nu_{\text{eff}})}{(1-g^2)\mathbf{E}+\nu_{\text{eff}}g^2(\mathbf{E}-\mathbf{K})} -\frac{1}{2}\frac{(1-g^2)(1-2\nu_{\text{eff}})}{(1-g^2)\mathbf{E}+\nu_{\text{eff}}(g^2\mathbf{K}-\mathbf{E})}\right]. \tag{58}$$

It is interesting to observe that, as for 2D elasticity, there is an exponential dependence upon the crack and, therefore, the overall mechanical behavior is strongly affected by cracks. Solutions of Eqs. (57) and (58) are represented in Fig. 9. Drawing a comparison among these results and those obtained in 2D elasticity, we may observe that the effect of the degradation is stronger in this latter case (at the same crack density). Interesting enough, in 3D elasticity no unconventional effects in the degradation process are exhibited.

VI. CONCLUSIONS

In this work we have analyzed the effects of the orientational order/disorder of elliptic cracks in a homogeneous solid and we have described an explicit procedure providing a thorough description of the mechanical behavior of a multicracked medium. We have found the proper definitions of some order parameters, in such a way to predict the macroscopic elastic properties as function of the state of microscopic order. In particular, we have found that two order parameters are able to describe the orientational distribution of cracks, both with orthorhombic and transversely isotropic symmetries.

As results of great practical relevance, we have determined the effective stiffness tensor of a multicracked material in terms of the crack microstructure and distribution (in the case of small crack density). Under the additional hypothesis of isotropic distribution of cracks, we have also generalized our results to the regime of large crack density using the iterative homogenization method and the differential scheme.

ACKNOWLEDGMENTS

We acknowledge financial support by MUR under project PON -"CyberSar" (OR 7). One of us (L.C.) also acknowledges support by INdAM "F. Severi" through the research project "Mathematical challenges in nanomechanics."

APPENDIX A: ESHELBY TENSOR DEFINITION

We consider the half-axes $a_1>a_2>a_3>0$ aligned along the axes x_1,x_2,x_3 of the references frame. Therefore, we define two aspect ratios as $0<e=a_3/a_2<1$ and $0<g=a_2/a_1<1$. They completely describe the shape of the inclusion. The so-called depolarizing factors are defined as follows[25]

$$I_3 = \frac{4\pi}{1-e^2}-\frac{4\pi e}{(1-e^2)\sqrt{1-e^2g^2}}\mathbb{E}(v,q),$$

$$I_2 = \frac{4\pi e(1-e^2g^2)}{(1-e^2)(1-g^2)\sqrt{1-e^2g^2}}\mathbb{E}(v,q) -\frac{4\pi eg^2}{(1-g^2)\sqrt{1-e^2g^2}}\mathbb{F}(v,q)-\frac{4\pi e^2}{1-e^2},$$

$$I_1 = \frac{4\pi eg^2}{(1-g^2)\sqrt{1-e^2g^2}}[\mathbb{F}(v,q)-\mathbb{E}(v,q)], \tag{A1}$$

where the quantities v and q are defined as follows

$$v=\arcsin\sqrt{1-e^2g^2}, \quad q=\sqrt{\frac{1-g^2}{1-e^2g^2}}. \tag{A2}$$

In the previous expressions we have used the incomplete elliptic integrals of the first kind $\mathbb{F}(v,q)$ and the second kind $\mathbb{E}(v,q)$[32]

$$\mathbb{F}(v,q)=\int_0^v\frac{d\alpha}{\sqrt{1-q^2\sin^2\alpha}}=\int_0^{\sin v}\frac{dx}{\sqrt{(1-x^2)(1-q^2x^2)}},$$

$$\mathbb{E}(v,q) = \int_0^v \sqrt{1 - q^2 \sin^2\alpha}\, d\alpha = \int_0^{\sin v} \frac{\sqrt{1-q^2x^2}}{\sqrt{1-x^2}} dx. \tag{A3}$$

Moreover, we define the functions $\mathbf{K}(q)$ and $\mathbf{E}(q)$ called complete elliptic integrals of the first kind and of the second kind, respectively, used in the main text for several developments[33]

$$\mathbf{K}(q) = \mathbb{F}\left(\frac{\pi}{2}, q\right), \quad \mathbf{E}(q) = \mathbb{E}\left(\frac{\pi}{2}, q\right), \tag{A4}$$

where $\mathbb{F}$ and $\mathbb{E}$ are the incomplete elliptic integrals defined in Eq. (A3). The following parameters are necessary for the following calculations[25]

$$I_{12} = \frac{I_2 - I_1}{1-g^2}, \quad I_{13} = \frac{I_3 - I_1}{1-e^2g^2}, \quad I_{23} = \frac{I_3 - I_2}{g^2(1-e^2)},$$

$$I_{11} = \frac{1}{3}\frac{I_1(e^2g^4 - 2e^2g^2 - 2g^2 + 3) + I_2g^2(e^2g^2 - 1) + I_3e^2g^2(g^2 - 1)}{(1-g^2)(1-e^2g^2)},$$

$$I_{22} = \frac{1}{3}\frac{I_1(1-e^2) + I_2(2e^2g^2 - 3g^2 + 2 - e^2) + I_3e^2(g^2 - 1)}{g^2(1-e^2)(1-g^2)},$$

$$I_{33} = \frac{1}{3}\frac{I_1(1-e^2) + I_2(1-e^2g^2) + I_3(1 - 2e^2g^2 + 3e^4g^2 - 2e^2)}{e^2g^2(1-e^2)(1-e^2g^2)}. \tag{A5}$$

The generic Eshelby tensor is given, in Voigt notation, by

$$\tilde{\mathcal{S}} = \begin{bmatrix} M & 0 \\ 0 & N \end{bmatrix}, \tag{A6}$$

where the submatrices can be written as follows

$$M = \begin{bmatrix} \frac{3I_{11} + (1-2\nu)I_1}{8\pi(1-\nu)} & \frac{g^2I_{12} - (1-2\nu)I_1}{8\pi(1-\nu)} & \frac{e^2g^2I_{13} - (1-2\nu)I_1}{8\pi(1-\nu)} \\ \frac{I_{12} - (1-2\nu)I_2}{8\pi(1-\nu)} & \frac{3g^2I_{22} + (1-2\nu)I_2}{8\pi(1-\nu)} & \frac{e^2g^2I_{23} - (1-2\nu)I_2}{8\pi(1-\nu)} \\ \frac{I_{13} - (1-2\nu)I_3}{8\pi(1-\nu)} & \frac{g^2I_{23} - (1-2\nu)I_3}{8\pi(1-\nu)} & \frac{3e^2g^2I_{33} + (1-2\nu)I_3}{8\pi(1-\nu)} \end{bmatrix}, \tag{A7}$$

$$N = \begin{bmatrix} N_{11} & 0 & 0 \\ 0 & N_{22} & 0 \\ 0 & 0 & N_{33} \end{bmatrix}, \tag{A8}$$

where

$$N_{11} = \frac{(1+g^2)I_{12} + (1-2\nu)(I_1 + I_2)}{8\pi(1-\nu)},$$

$$N_{22} = \frac{g^2(1+e^2)I_{23} + (1-2\nu)(I_2 + I_3)}{8\pi(1-\nu)},$$

$$N_{33} = \frac{(1+e^2g^2)I_{13} + (1-2\nu)(I_1 + I_3)}{8\pi(1-\nu)}. \tag{A9}$$

APPENDIX B: TENSOR $\tilde{\mathcal{G}}$ FOR TRANSVERSELY ISOTROPIC SYMMETRY

The tensor $\tilde{\mathcal{G}}$, as described in Sec. V A, has the same structure of the tensor $\tilde{\mathcal{W}}$ defined in Eq. (42). A complete list of the entries of such a tensor is given below

$$\mathcal{G}_{11} = \frac{4}{315}\frac{\pi\alpha g^2(1-\nu)(14-9T-5S)(1-g^2)}{(1-g^2)\mathbf{E}+\nu(g^2\mathbf{K}-\mathbf{E})} + \frac{4}{315}\frac{\pi\alpha g^2(1-\nu)(14-9T-5S)(1-g^2)}{(1-g^2)\mathbf{E}+\nu g^2(\mathbf{E}-\mathbf{K})} + \frac{8}{315}\frac{\pi\alpha g^2(1-\nu)[7(3-\nu)-9T(1-2\nu)-5S(6-5\nu)]}{\mathbf{E}(1-2\nu)}, \tag{B1}$$

$$\mathcal{G}_{12} = \frac{4}{315}\frac{\pi\alpha g^2(1-\nu)(10S-3T-7)(1-g^2)}{(1-g^2)\mathbf{E}+\nu(g^2\mathbf{K}-\mathbf{E})} + \frac{4}{315}\frac{\pi\alpha g^2(1-\nu)(10S-3T-7)(1-g^2)}{(1-g^2)\mathbf{E}+\nu g^2(\mathbf{E}-\mathbf{K})} + \frac{8}{315}\frac{\pi\alpha g^2(1-\nu)[7(1+3\nu)+3T(1-2\nu)-5S(2+3\nu)]}{\mathbf{E}(1-2\nu)}, \tag{B2}$$

$$\mathcal{G}_{13} = \frac{4}{315}\frac{\pi\alpha g^2(1-\nu)(12T-5S-7)(1-g^2)}{(1-g^2)\mathbf{E}+\nu(g^2\mathbf{K}-\mathbf{E})} + \frac{4}{315}\frac{\pi\alpha g^2(1-\nu)(12T-5S-7)(1-g^2)}{(1-g^2)\mathbf{E}+\nu g^2(\mathbf{E}-\mathbf{K})} + \frac{8}{315}\frac{\pi\alpha g^2(1-\nu)[7(1+3\nu)-12T(1-2\nu)+5S(1-9\nu)]}{\mathbf{E}(1-2\nu)}, \tag{B3}$$

$$\mathcal{G}_{31} = \frac{4}{315}\frac{\pi\alpha g^2 v(1-\nu)(12T-5S-7)(1-g^2)}{(1-g^2)\mathbf{E}+\nu(g^2\mathbf{K}-\mathbf{E})} + \frac{4}{315}\frac{\pi\alpha g^2(1-\nu)(12T-5S-7)(1-g^2)}{(1-g^2)\mathbf{E}+\nu g^2(\mathbf{E}-\mathbf{K})} + \frac{8}{315}\frac{\pi\alpha g^2(1-\nu)[7(1+3\nu)-12T(1-2\nu)+5S(1+12\nu)]}{\mathbf{E}(1-2\nu)}, \tag{B4}$$

$$\mathcal{G}_{33} = -\frac{8}{315}\frac{\pi\alpha g^2(1-\nu)(12T-5S-7)(1-g^2)}{(1-g^2)\mathbf{E}+\nu(g^2\mathbf{K}-\mathbf{E})} - \frac{8}{315}\frac{\pi\alpha g^2(1-\nu)(12T-5S-7)(1-g^2)}{(1-g^2)\mathbf{E}+\nu g^2(\mathbf{E}-\mathbf{K})} + \frac{8}{315}\frac{\pi\alpha g^2(1-\nu)[7(3-\nu)+24T(1-2\nu)+10S(6-5\nu)]}{\mathbf{E}(1-2\nu)}, \tag{B5}$$

$$\mathcal{G}_{55} = \frac{2}{105}\frac{\pi\alpha g^2(1-\nu)(14+16T+5S)(1-g^2)}{(1-g^2)\mathbf{E}+\nu(g^2\mathbf{K}-\mathbf{E})} + \frac{2}{105}\frac{\pi\alpha g^2(1-\nu)(14+16T+5S)(1-g^2)}{(1-g^2)\mathbf{E}+\nu g^2(\mathbf{E}-\mathbf{K})} + \frac{16}{315}\frac{\pi\alpha g^2(1-\nu)(7-12T+5S)}{\mathbf{E}}. \tag{B6}$$

This complete list of expressions allows us to obtain the effective stiffness tensor $\tilde{\mathcal{C}}_{\text{eff}}$ by applying Eq. (17). The final results are given in Eqs. (46)–(51) providing the effective Hill parameters.

*stefano.giordano@dsf.unica.it
†luciano.colombo@dsf.unica.it

[1] A. A. Griffith, Philos. Trans. R. Soc. London, Ser. A **221**, 163 (1920).
[2] K. B. Broberg, *Cracks and Fracture* (Academic Press, London, 1999).
[3] A. Mattoni, L. Colombo, and F. Cleri, Phys. Rev. Lett. **95**, 115501 (2005).
[4] M. Kachanov and I. Sevostianov, Int. J. Solids Struct. **42**, 309 (2005).
[5] *Heterogeneous Media: Micromechanics Modeling Methods and Simulations*, edited by K. Z. Markov and L. Preziozi (Birkhauser, Boston, 2000).
[6] Z. Hashin and S. Shtrikman, J. Mech. Phys. Solids **10**, 335 (1962).
[7] L. J. Walpole, Adv. Appl. Mech. **11**, 169 (1981).
[8] Z. Hashin, J. Appl. Mech. **50**, 481 (1983).
[9] M. Avellaneda, Commun. Pure Appl. Math. **40**, 527 (1987).
[10] R. McLaughlin, Int. J. Eng. Sci. **15**, 237 (1977).
[11] S. Giordano, Eur. J. Mech. A/Solids **22**, 885 (2003).
[12] T. Pointer, E. Liu, and J. A. Hudson, Geophys. J. Int. **142**, 199 (2000).
[13] S. R. Tod, Geophys. J. Int. **146**, 249 (2001).
[14] R. K. Nalla, J. H. Kinney, and R. O. Ritchie, Biomaterials **24**, 3955 (2003).
[15] N. A. Danova, S. A. Colopy, C. L. Radtke, V. L. Kalscheur, M. D. Markel, R. Vanderby, Jr., R. P. McCabe, A. J. Escarcega, and P. Muir, Bone (N.Y.) **33**, 197 (2003).
[16] S. Giordano and L. Colombo, Phys. Rev. Lett. **98**, 055503 (2007).
[17] S. Giordano and L. Colombo, Eng. Fract. Mech. **74**, 1983 (2007).
[18] B. Budiansky and R. J. O'Connell, Int. J. Solids Struct. **12**, 81 (1976).
[19] J. A. Hudson, Math. Proc. Cambridge Philos. Soc. **88**, 371

(1980).
[20] M. Kachanov, Appl. Mech. Rev. **45**, 305 (1992).
[21] I. Sevostianov and M. Kachanov, Mater. Sci. Eng., A **297**, 235 (2001).
[22] I. Sevostianov, M. Kachanov, J. Ruud, P. Lorraine, and M. Dubois, Mater. Sci. Eng., A **386**, 164 (2004).
[23] J. D. Eshelby, Proc. R. Soc. London, Ser. A **241**, 376 (1957).
[24] J. D. Eshelby, Proc. R. Soc. London, Ser. A **252**, 561 (1959).
[25] T. Mura, *Micromechanics of Defects in Solids* (Kluwer Academic, Dordrecht, 1987).
[26] Q. Yang, W. Y. Zhou, and G. Swoboda, Trans. ASME, J. Appl. Mech. **68**, 740 (2001).
[27] S. Giordano and L. Colombo, Phys. Rev. B **76**, 174120 (2007).
[28] We remark that these first order terms are proportional to $1/e$ since the tensor $[\tilde{I}-\tilde{\mathcal{S}}]$ is singular for vanishing e. On the other hand, higher order terms disappear in the limit $e \to 0$.
[29] R. Lakes, Science **235**, 1038 (1987).
[30] B. Shafiro and M. Kachanov, J. Appl. Phys. **87**, 8561 (2000).
[31] The probability density is symmetrical with respect to $\theta=\pi/2$ and fulfills the following limiting cases: If $\chi \to -\infty$, then $f(\theta) \to 1/2\delta(\theta)+1/2\delta(\theta-\pi)$ (order) and $C_2=C_4=1$; if $\chi=0$, then $f(\theta)=1/2\sin(\theta)$ (disorder), $C_2=1/3$ and $C_4=1/5$; finally, if $\chi \to +\infty$, then $f(\theta)=\delta(\theta-\pi/2)$ and all the cracks have the normal vector orthogonal to the x_3 axis ($C_2=C_4=0$).
[32] I. S. Gradshteyn and I. M. Ryzhik, *Table of Integrals, Series, and Products* (Academic Press, San Diego, 1965).
[33] M. Abramowitz and I. A. Stegun, *Handbook of Mathematical Functions* (Dover, New York, 1970).